Object Extraction from Architecture Scenes through 3D Local Scanned Data Analysis

Xiaojuan NING, Yinghui WANG
Department of Computer Science and Engineering, Xi'an University of technology, Xi'an, 710048, China
ningxiaojuan@xaut.edu.cn

***Abstract*—Terrestrial laser scanning becomes a standard way for acquiring 3D data of complex outdoor objects. The processing of huge number of points and recognition of different objects inside become a new challenge, especially in the case where objects are included. In this paper, a new approach is proposed to classify objects through an analysis on shape information of the point cloud data. The scanned scene is constructed using k Nearest Neighboring (k-NN), and then similarity measurement between points is defined to cluster points with similar primitive shapes. Moreover, we introduce a combined geometrical criterion to refine the over-segmented results. To achieve more detail information, a residual based segmentation is adopted to refine the segmentation of architectural objects into more parts with different shape properties. Experimental results demonstrate that this approach can be used as a robust way to extract different objects in the scenes.**

***Index Terms*—Terrestrial Laser Scanner, Point Cloud Segmentation, Similarity Measurement, Nearest Neighboring Graph.**

I. INTRODUCTION

The acquisition, processing and reconstruction of 3D large scenes in the real world have received more attentions over the last few years. Represented as unorganized 3D point cloud data (short for PCD), the digital information of scenes generally contain various object information with different geometric shapes. In the context of urban scenes, parks and forest stands, object extractions offer a wide field of applications including:

Architectural Reconstruction. Existing architectures extraction, as a complete entity with parametric level of composition details show interest for professional and entertainment uses. It is of high interest in city planning, inventories, virtual tourism and cultural heritage documentation.

Tree Modeling. Vegetation extraction shows interest in planning also. Vegetation inventories and their updates is a clear target. Moreover, in Life sciences studies, the extraction of single plants can involve further 3D measurements, such as trunk diameters, crown height and sizes, plant structure up to age estimation.

The most important issue is that how to extract and classify different shapes from the unorganized sampled data, which is also a fundamental task in computer graphics, computer vision and reverse engineering. There is a lot of research work on the techniques of dealing with extraction and segmentation from imperfect point clouds [1]-[4]. Many methods are proposed, such as RANSAC [5]-[8], Hough transform [9]-[12] and region growing method [13]-[18]. However RANSAC can only detect the small shapes in large point clouds and the number of required shape hypothesis is prohibitively large. 3D HT is time-consuming and high dimensional parameter domain becomes a major drawback which is not suitable for huge point cloud data.

The raw point cloud, as an output format of laser scanner, often contains more redundant information and no interpretation of the data which makes it difficult to process in an efficient manner. On the other side it also shows missing areas due to occlusions. Although there are various methods based on mesh data, it is not feasible to convert the point cloud into mesh directly since there are much more noisy data. Therefore in this paper, our work focused on the extraction of objects with different shapes and geometric information from unorganized point cloud data, especially the trees, architecture, pillars and the street lamp, etc.

Figure 1(a) displays the panoramic image of scanned scenes, and Figure 1(b) is the point cloud data of scanned partial scenes from the local box in red in Figure 1(a). In addition, the range image of Figure 1(b) is given in Figure 1(c). Observed that most of the trees, lamp-post and notice board may have a certain distances away from the architecture, and for the architecture part, the windows may have a certain distance away from the wall, the wall and windows of the architecture all displayed as planar shape. In this case, a local connectivity based segmentation method is adopted, and the similarity of two vertices is measured by a weighted value. Meanwhile, a merging process between clusters is implemented to refine and improve the results if the results are not satisfactory.

In this paper, our main contribution is the extraction of various objects in the scanned urban scenes. Our method can not only extract the large objects existed in the scenes, but the detailed part of each object can also be acquired.

II. ALGORITHM OVERVIEW

We are interested in objects existed in complex urban scenes that range in size from architecture to street lamp-post, even the windows and doors. Our algorithm operates on 3D raw point clouds and returns the points that belong to an object. The whole process of our approach is described as follows summarized with the specific flowchart in Figure 2.

(1) Construct the k-nearest neighbor graph (k-NNG) for the input point clouds. Compute the normal for all points which will be used as one of the criteria for similarity will

This work is supported in part by National Natural Science Foundation of China under Grant No.61072151, No.61272284; and in part by Shaanxi Educational Science Research Plan under Grant No.09JK628, No.2010JK734; and in part by Shaanxi Science Research Plan under Grant No.2011K06-35, and in part by Xi'an Science Research Plan under Grant No.CX1252 (3), and in part by Xi'an BeiLin Science Research Plan under Grant No.GX1212.

Digital Object Identifier 10.4316/AECE.2012.03011

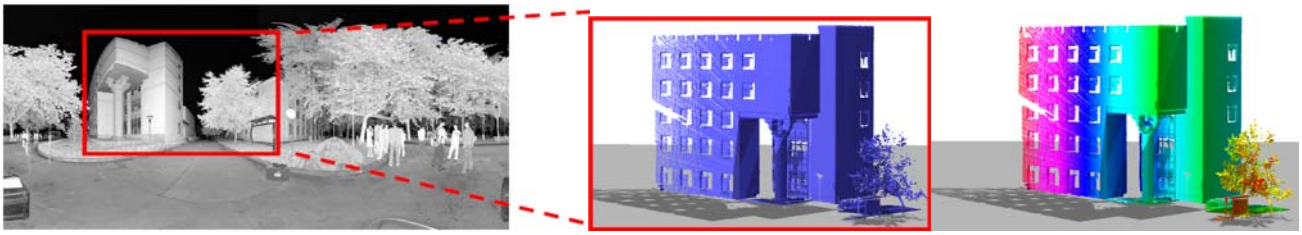

(a) (b) (c)

Figure 1. Scanned Scenes. (a) Panoramic Image of Scanned Scenes, (b) Point Cloud Data, (c) Range Image

be used as one of the criteria for similarity measurement detailed further in section 3.3.

(2) Find the neighboring points according to their k-NNG, and cluster together the points with consistent similarity and local connectivity. The scenes are segmented into several different, intuitive and meaningful clusters;

(3) Define a confidence rate C_{Rate} (defined in section 4.2) in order to determine the final number of clusters that will be combined or merged. Merge the clusters according to the fusion strategy, and label all points that belong to each object to obtain satisfactory segmentation results.

(4) Residual based segmentation algorithm is implemented on the obtained complete architecture, and the detailed part can be separated which is useful for further classification and recognition.

III. Similarity-Based Clustering

Inspired by the graph-based image segmentation [19], we involve the graph theory into point cloud domain.

3.1 Construction of KNN Graph

Given the raw point cloud data P={p_1, p_2, p_3}, let G=(P,E) be an undirected graph with vertices $p \in P$. Assume point $\{p_i(x_i,y_i,z_i)\}_{i=1:n}$ and its neighboring points $\{q_j(x_j,y_j,z_j)\}_{j=1:k}$ within a given distance, there will be an edge E_{ij} connecting each two points. The length of the edge is the Euclidean distance of the two points. The local neighborhood relationships between the data point are implemented using k nearest neighbor graphs (k-NNG) of point clouds. Connect p_i and q_j with an undirected edge if p_i is among the k nearest neighbors of q_j or if q_j is among the k nearest neighbors of pi. Here k-NNG is constructed using ANN library (Approximate Nearest Neighbor), in which k-d tree, a binary tree of k dimensional keys, is adopted to organize the data to speed up the search.

3.2 Normal Estimation

The method in [20] made use of a local weighted plane fitting method to compute the surface normal of each point, and then refined it by vector voting. This method can obtain more accurate normal vector than PCA method in [21], which is effective for further segmentation of different primitive shape including not only planes but also other cylinder shapes.

Consider that p is a point in the point cloud data and $n(p)$ is the normal vector at point p. Then initial normal n_1 can be calculated through minimizing the weighted square distance between neighboring points $q_i(x_i,y_i,z_i)(i=1,2,..k)$ and a plane **H** passing through p, $H=\{x \mid < x-p, n >= 0, x \in R_3\}$, so $n(p)$ satisfies

$$\min_{\|n\|=1} \sum <q_i-p, n_1>^2 \omega\left(\frac{\|q_i-p\|}{d}\right) \quad (1)$$

where weighted function $w(x) = (1-x)^4(1+4x)$. The obtained initial normal n_1 should be refined by normal voting according to the optimization function

$$\max_{\|n\|=1} \sum <m,n>^2 \omega\left(\frac{\|q_i-p\|}{d}\right) \quad (2)$$

where m_i is the most likely normal for every neighbor points q_i. The solution $n(p)$ is accepted as the refined normal direction at point p.

3.3 Similarity Measurement

The method in our previous work [22] was used to segment the trees in the scene, which is based on k nearest neighboring clustering. The raw point cloud data P is clustered into m ($m<N$) patches C_1, C_2, ..., C_m using k nearest neighboring clustering. That is to say, the point pi and its neighborhood q_1, q_2, ..., q_k within an assumed threshold d_{th} can be clustered as one segment since the points belonging to one object should have smaller distance than those belonging to two objects.

Here it cannot get satisfactory segmentation result from k-NN clustering, because many clusters which are close to each other or noisy points connecting them can be segmented into the same regions by mistake. After clustering the scenes may be segmented into many patches, some of which can represent a complete object, but some objects may be clustered into several patches. Obviously, it may easily lead to under segmentation and over segmentation results not only because the choice of k depends on the density of the scanned data but the clustering is also effected by the scanning order. All of these would make random and unsatisfactory results.

The clustering of scanned scenes in [22] is displayed in Figure 3. The segmentation results are different since k impacts drastically the segmentation results. This is why the similarity measurement is proposed instead of this method in this paper. In order to avoid under segmentation, the normal of each point which is obtained in previous section will be used as one similarity measurement of each two points. A weight value is defined as $W(p_i,q_i)$ for each point pair (see Figure 3) in the following:

$$W(p_i,q_i) = \begin{cases} 1 & if\ d^* < d_{th}, N^* < \theta_{th} \\ 0 & otherwise \end{cases} \quad (3)$$

where $d^* = d(p_i,q_j)$ which is the Euclidean distance

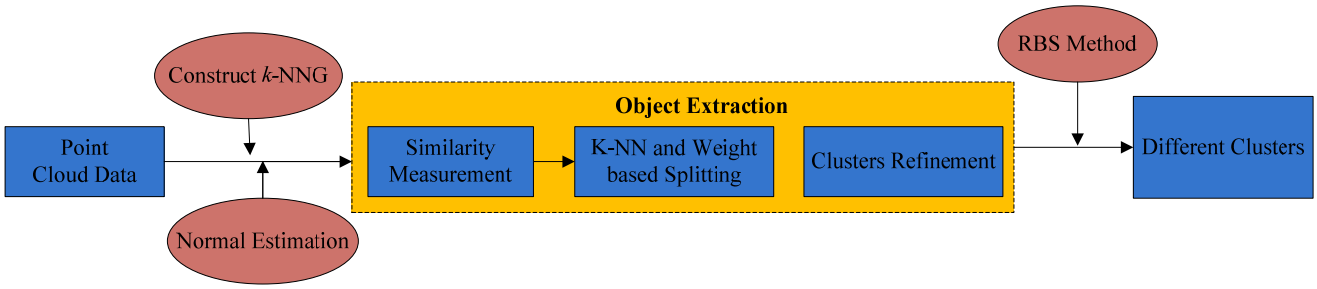

Figure 2. Diagram of Our Algorithm

.

between point p_i and q_j, $N^* = N(p_i, q_j)$ which denotes the angle between normal vector n_{p_i} and n_{q_j}.

In our experiments, the threshold d_{th} is equal to the minimum distance $d_{\min}$ multiplied by a coefficient determined by users (which depends on the density of sampling data), and θ_{th} means that two normal deviate no more than the angle θ_{th} (10-15) degrees. In Figure 4, the red line connecting pi and its neighboring points q_j is an edge denoted as E, and the weight $W(p_i, q_i)$ for each edge ***E*** represents whether the two points belong to one cluster or not. The dotted line means that the relation (whether there is an edge) between the two points should be re-determined. Based on the similarity measurement, the clustering result is shown in section 3.4.

3.4 Clustering

The steps of the segmentation algorithm based on similarity measurement are summarized as follows:

(1) Specify the k nearest neighboring points with ANN; Compute normal n_p of every point; determine the distance threshold d_{th} and angle threshold θ_{th};

(2) Start from seed point (the point has minimum curvature) in the raw PCD, and search for its k nearest neighboring points; Cluster those points which have the same similarity with the seed point and a label is also delivered to each point in the cluster;

(3) Process another point and repeat the step (2) until all the points in the raw PCD are labeled and segmented.

(a) k=30

(b) k=100

Figure 3. Segmentation based on KNN [22].

The clustering result of the scanned scenes based on similarity measurement is displayed in Figure 4. Nevertheless, there is also some inaccurate place or unsatisfactory results. Therefore they are required to be refined in order to make better segmentation results.

IV. Fusion and Refinement

In our method, we prefer over segmentation than under segmentation. For the obtained over segmentation results, further fusion process is required to implement satisfactory results. Therefore it is necessary to combine the small patches to obtain a complete one. Mathematically, the clusters are determined by minimizing an objective function. The fusion process is based on a mixed normal and distance criterion.

4.1 Fusion Strategy

In fact, the fusion process is to merge those points belonging to one cluster yet segmented by mistake. In order to predicate whether two clusters can be merged into one, a predicated expression is shown below. The fusion strategy must comply with the condition.

$$f(C_i^*, C_j^*) = \min_{n \geq i > j \geq 1} \{w \cdot d(C_i, C_j) + (1-w) \cdot \theta(C_i, C_j)\} \quad (4)$$

where $d(C_i, C_j)$ is the Euclidean distance between cluster C_i and C_j. $\theta(C_i, C_j)$ is the angle between the normal n_{C_i} of cluster C_i and n_{Cj} of cluster C_j. n_{C_i} is determined by $n_{C_i} = \frac{1}{\tau}\sum_{\mu=1}^{\tau} n_{p_\mu} (p \in C_i)$. The coefficient $w \in [0,1]$ is designed according to objects "type": if the fusion is based on normal only, $w = 0$; respectively $w = 1$ gives full prior to distance criteria. Following the fusion strategy, the clusters are merged in section 4.3.

4.2 Cluster Number Determination

In addition, a "satisfactory" fusion criterion is defined, as the quotient between inter and intra cluster distances. The distances between two clusters denoted as *interClusterDist* and the squared distances between the points and the corresponding centroid in one cluster denoted as *intraClusterDist*.

$$interClusterDist(C_i, C_j) = \min D(B_{C_i}, B_{C_j}) \quad i \neq j \quad (5)$$

where $D(B_{C_i}, B_{C_j})$ denotes the distance between the bounding box of cluster C_i and C_j. By calculating the distance between the eight vertices in each bounding box, the *intraClusterDist* can be defined as:

$$intraClusterDist(C) = \min_{p,q \in C}\{D(p,q)\} \quad (6)$$

Therefore if C_i and C_j are combined into cluster C^*, then

$$intraClusterDist(C^*) = \min\{D((p_m)_{C_i}, (q_n)_{C_j})\}_{C_i \cup C_j = C^*} \quad (7)$$

where $(p_m)_{(C_i)}$ are the points in cluster C_i, and $(q_n)_{(C_j)}$ denotes points in cluster C_j.

A confidence rate $C_{Rate}(C_i, C_j)$ is designed to help us to determine if the two clusters can be merged or not. It is defined as

$$C_{Rate}(C_i, C_j) = \frac{intraClusterDist(C_i)}{interClusterDist(C_i, C_j)} \quad (8)$$

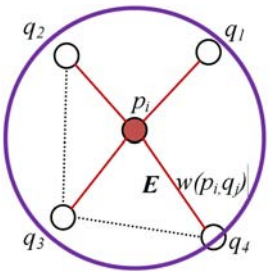

Figure 4. Weights of Neighboring Point.

4.3 Fusion Process

Generally the architecture is the most critical and largest object in the scanned outdoor scene; therefore in this section we display the whole process to acquire complete architecture as follows.

(1) Start from the largest cluster C_i^*; initialize the strategy function by setting w = 1 and obtain a cluster C_j^*; Determine whether or not the two cluster have similar normal;

(2) If the two clusters C_i^* and C_j^* can be merged (the normal difference between two clusters is less than θ_{th}, then we calculate the C_{Rate} before and after C_i^* and C_j^* are merged respectively. It mainly compares *intra-ClusterDist* variation before and after merging, i.e. $C_{Rate}(C_i^*, C_j^*) = \frac{intraClusterDist(C_i^*)}{interClusterDist(C_i^*, C_j^*)}$ and $C_{Rate}(C_i^* \cup C_j^*, C_j^*) = \frac{intraClusterDist(C_i^* \cup C_j^*)}{interClusterDist(C_i^*, C_j^*)}$. If the relative change between $C_{Rate}(C_i^* \cup C_j^*, C_j^*)$ and $C_{Rate}(C_i^*, C_j^*)$ have smaller variation, i.e $\delta_c^{c'} = \frac{C_{Rate}(C_i^*, C_j^*)}{C_{Rate}(C_i^* \cup C_j^*), C_j^*)}$, if $\delta_c^{c'}$ is more than 85% then they can be merged; else find another cluster close to C_i^* and continue (2);

(3) Merge the two clusters and the initial clusters number are decreased; find next cluster close to C_i^* from the remaining clusters and continue this process;

(4) Return final results C_i^* after fusion.

4.4 Residual Based Segmentation

After segmentation and fusion processes, the scanned views can be registered into several object classes such as building facade, ground, pillar, notice board etc. However, on architectural part, more detailed components are required to be detected on facades.

Figure 5. Clustering Results.

The residual based segmentation [21] is adopted to extract different components of the architecture since the walls, windows and doors have their own characteristic feature. A brief description is provided here for its strong relevance with this paper. This method starts by choosing a seed point with minimum residual value (the smaller the residual is, the more flat the plane which the point located in). The algorithm finds the neighboring unclassified points and tests if they can be fitted to the plane which seed point located in. If so, then it grows the next unclassified seed point. The results are displayed in Figure 6.

V. Experimental Results

Several different point cloud data of the large scenes in real world are executed with our method. All experiments are implemented on a PC with INTEL Core ^{TM}2 CPU, and 2G memory.

5.1 Data Acquisition

These scans of the laboratory in Xi'an university of technology (Data 1), the facades of the buildings in CASIA (Data 2) and another two buildings from Yan'an city (Data 3 and Data 4) were collected by Faro Scanner. Within our investigations, a standard digital camera was used for image collections, while Faro scanner LS 880 HE40 was used for measurement. This scanner is based on a phase shift laser operating at a wavelength of 785nm. It is able to acquire a scene with a field of view of up to 360° horizontal and 320° vertical in a single scan. The scanned data 1 is a typical urban scene which consists of exactly 1224422 points, in which there are architecture, ground, trees, lamp-post and notice board, etc. The original point cloud data is displayed in Figure 1(b) and also the range image is represented as in Figure 1(c). The scanned data 2 consists of 51355 points, in which there are architecture, trees and many noisy points.

5.2 Results

The experiments are carried out on the scanned scenes including different objects. One can thus access the robustness and the efficiency of the proposed approach.

We can see from Figure 6 that walls with different orientation, windows, and doors are split more accurately, which is beneficial for further object recognition. Figure 6(b) display the results by using the proposed clustering method, and Figure 6(c)-(f) illustrate the detail segmentation using residual based method. In addition, the deleted noisy points are displayed in Figure 7, which indicated that they may contain not only sparse points but the leaves.

Another example for segmentation of the objects using our approach is shown in Figure 8. The data contain 51,356 points which are composed of several trees, a main building and some other incomplete building part. The trees can be separated from each other and from the buildings since there are more distances away from the building and the similarity between the building and trees is lower. Detail information for trees can also be acquired by segmentation in Figure 8(b). From left to right, the tree respectively contains 13,844, 7,438 and 1,081 points.

The segmentation based on similarity measurement typically needs about 15~25 seconds for 100000~200000 points. The feature extraction may take more or less 1 second. Classification and recognition processes can be finished within a matter of seconds even for complex models. All times were recorded on a standard PC with 2GHz.

5.3 Limitation of Our Approach

Although our method can effectively extract the objects from the large scanned scenes and also can classify and recognize the objects from each other, there are still a few limitations reflecting on the implementation of our approach. On one hand, it cannot handle the complex building, particularly the one with more windows but small size walls which may result in small patches of the wall. On the other hand, it seems that the classification is at the limit of what can be done with our approach of segmentation.

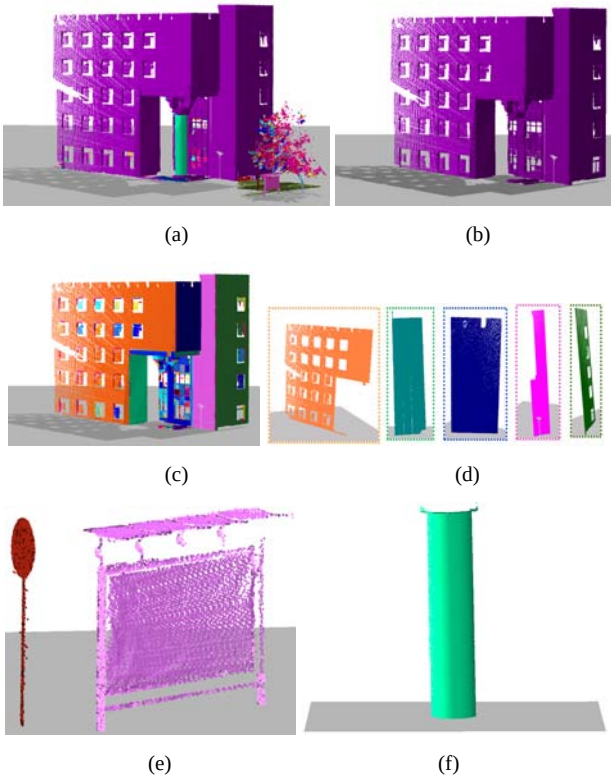

(a) (b) (c) (d) (e) (f)

Figure 6. Segmentation Results On Data with 1224422 points. (a) Refinement Results, (b) Building Part, (c) Residual based Segmentation, (d)-(f) illustrate the details.

VI. Conclusions

In this paper, we presented a similarity measurement based method to segment different types of objects in urban outdoor scenes. The segmentation involves cluster fusion combining balanced normal and distances. It is shown that the coupling of this approach with previous residual based segmentation method allows refining the segmented clusters into sub-objects with respect to a natural hierarchical classification. Experimental results demonstrate the effectiveness of our approach.

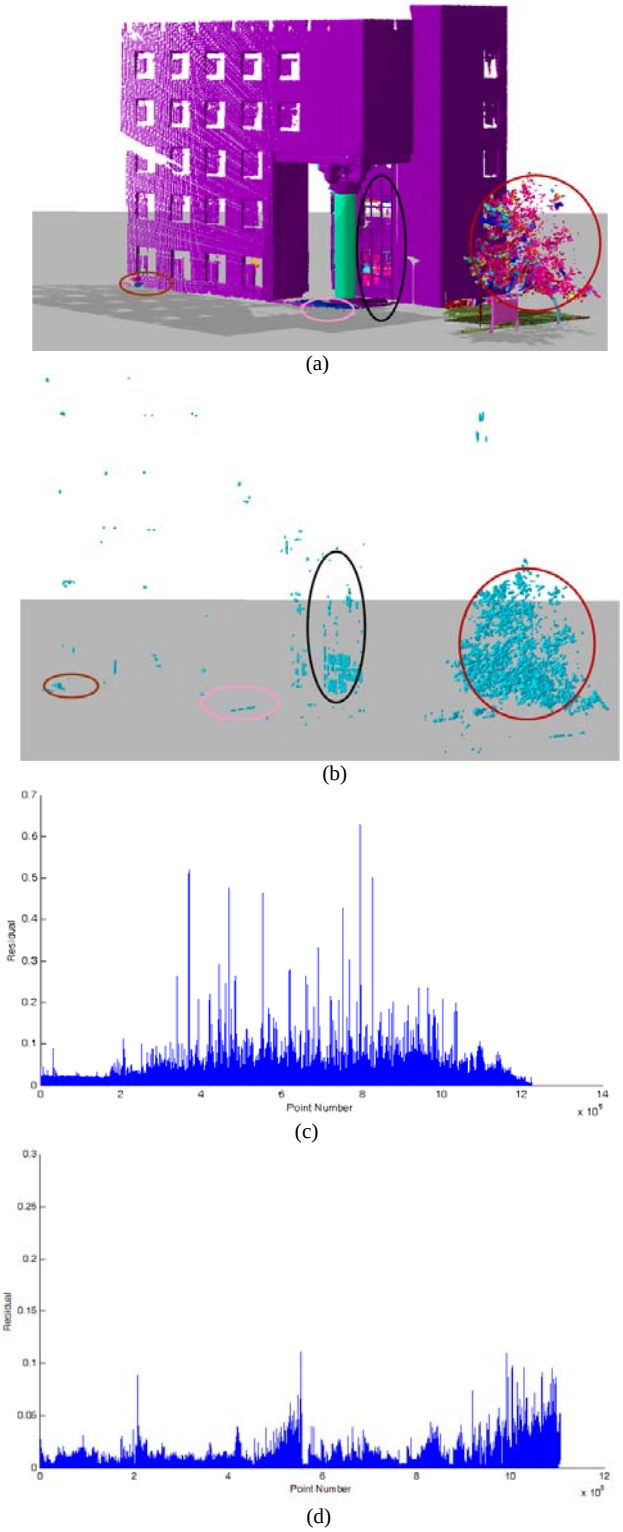

(a) (b) (c) (d)

Figure 7. Noisy points. (a) indicates the position that noisy points appeared in original data and the residual distribution, (b) is the corresponding noisy points, (c) and (d) represent corresponding residual distribution before and after noise removing.

The proposed approach shows generic capabilities. We did hereby focus on two clustering basic criteria - normal and distance, which were combined on a linear basis to refine the unsatisfactory results. This led us thus to define reference objects characterization criteria in respect with two basic features: objects showing high planar consistency

(buildings), or compact distances (foliage).

In addition, from another point of view there are two directions for future work. First, a more robust method should be generated for the detection and recognition of more primitive shapes. Second, our work could be focused mainly on architecture reconstruction keeping details more precisely and more concisely. The boundary points should be extracted and boundary curves should be fitted for an extraction of more features for automatic shape modeling of building facades. At midterm new basic segmentation criteria should be used to enforce segmentation. Specifically the reflectance value, available on many acquisition output could be a complementary criterion to be added to shape ones. Another idea is to link noise level with distance, so to link the fusion criteria to the distance.

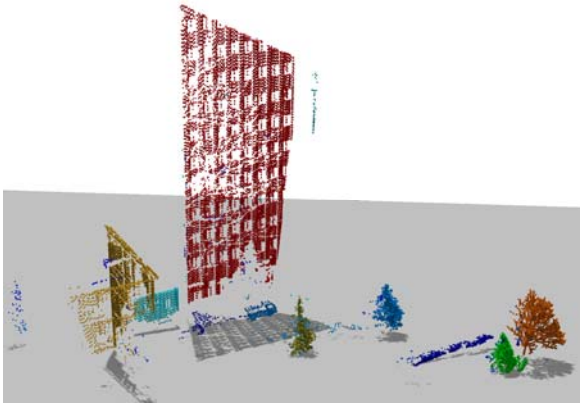

(a) The scanned scene

(b) The trees in the scene

Figure 8. Another example using our approach

REFERENCES

[1] Roth, G., Levine, M.D. "Extracting geometric primitives," *CVGIP: Image Underst*. 58(1), pp.1-22 (1993). [Online]. Available: http://dx.doi.org/10.1006/ciun.1993.1028.

[2] Phil Torr and Andrew Zisserman. "Robust computation and parameterization of multiple view relations," *In ICCV'98: Proceedings of the Sixth International Conference on Computer Vision*, Washington, DC, USA, 1998, pp.727. [Online]. Available: http://dx.doi.org/10.1109/ICCV.1998.710798.

[3] Torr, P.H.S., Zisserman, A. "Mlesac: a new robust estimator with application to estimating image geometry," *Comput. Vis. Image Underst.* 78(1), pp. 138-156, 2000. [Online]. Available: http://dx.doi.org/10.1006/cviu.1999.0832.

[4] Liang Xinhe, Liang Jin, Xiao Zhenzhong, Liu Jianwei, and Guo Cheng. "Study on Multi-Views Point Clouds Registration," *Adv. Sci. Lett*, 2011, 4, pp.2885-2889. [Online]. Available: http://dx.doi.org/10.1166/asl.2011.1573.

[5] Fischler, M.A., Bolles, R.C. "Random sample consensus: a paradigm for model fitting with applications to image analysis and automated cartography," *Commun. ACM.* 1981, 24, pp. 381-395 [Online]. Available: http://doi.acm.org/10.1145/358669.358692.

[6] Nistér, D. "Preemptive ransac for live structure and motion estimation," *Mach. Vision Appl*. 16(5), pp. 321-329, 2005. [Online]. Available: http://dx.doi.org/10.1007/s00138-005-0006-y.

[7] Ruwen Schnabel, Roland Wahl, and Reinhard Klein. "Shape detection in point clouds," *Technical Report CG-2006-2*, Universität Bonn, January 2006. [Online]. Available:

[8] Liangliang Nan, Andrei Sharf, Hao Zhang, DanielCohen-Or, and Baoquan Chen. "Smartboxes for interactive urban reconstruction," *ACM Trans. Graph*., 2010, 29, pp 93:1-93:10. [Online]. Available: 10.1145/1778765.1778830.

[9] Ballard, D.H. Generalizing the hough transform to detect arbitrary shapes. *Pattern recognition.* 1981, 13(2), pp .111-122, [Online]. Available: http://dl.acm.org/citation.cfm?id=33517.33574.

[10] George Vosselman, Er Dijkman. "3d building model reconstruction from point clouds and ground plans," *International Archives of Photogrammetry and Remote Sensing*, 2001, Volume XXXIV- 3/W4 (22-24), pp. 37-43.

[11] T Rabbani and F Van Den Heuvel. "Efficient hough transform for automatic detection of cylinders in point clouds," *In ISPRS WG III/3, III/4, V/3 workshop.* 2005, pp.60-65.

[12] Kourosh Khoshelham. "Extending generalized hough transform to detect 3d objects in laser range data," *Transform*, 2007, XXXV, pp. 206-210.

[13] P. J. Besl and R. C. Jain. "Segmentation through variable-order surface fitting," *IEEE Transaction on Pattern Analysis and Machine Intelligence*, 1988, 10(2), pp. 167-92. [Online]. Available: http://doi.ieeecomputersociety.org/10.1109/34.3881

[14] I. S. Chang and R. H.Park. "Segmentation based on fusion of range and intensity images using robust trimmed methods," *Pattern Reconition*, 2001, 34, pp. 1951-1962. [Online]. Available: http://dx.doi.org/10.1016/S0031-3203(00)00124-2.

[15] Klaus Köster and Michael Spann. "MIR: An approach to robust clustering application to range image segmentation," *IEEE Trans. Pattern Anal. Mach. Intell.*, 2000, 22(5), pp. 430-444. [Online]. Available: 10.1109/34.857001.

[16] Guoyu Wang, Zweitze Houkes, Guangrong Ji, Bing Zheng, and Xin Li. An estimation-based approach for range image segmentation: On the reliability of primitive extraction. *Pattern Recognition*, 2003, 36(1), pp.157-169, [Online]. Available: 10.1016/S0031-3203(02)00050-X.

[17] Jie Chen and Baoquan Chen. "Architectural modeling from sparsely scanned range data," *Int. J. Comput. Vision*, 2008, 78(2-3), pp.223-236. [Online]. Available: 10.1007/s11263-007-0105-5.

[18] Aleksey Golovinskiy and Thomas Funkhouser. "Min-cut based segmentation of point clouds," *In IEEE Workshop on Search in 3D and Video (S3DV) at ICCV*, 2009. [Online]. Available: 10.1109/ICCVW.2009.5457721.

[19] Pedro F. Felzenszwalb and Daniel P. Huttenlocher. "Efficient graph based image segmentation," *International Journal of Computer Vision*, 2004, 59(2), pp. 167-92. [Online]. Available: 10.1023/B:VISI.0000022288.19776.77.

[20] ZhangLin. Cheng,XiaoPeng Zhang. "Estimating differential quantities from point cloud based on a linear fitting of normal vectors," *Science in China Series F: Information Sciences*, 2009, 52, pp. 431-444. [Online]. Available: http://dx.doi.org/10.1007/s11432-009-0061-5.

[21] Xiaojuan Ning, Xiaopeng Zhang, and Yinghui Wang. Segmentation of architecture shape information from 3d point cloud. In The 8th ACM SIGGRAPH International Conference on VRCAI, 2009.12. [Online]. Available:10.1145/1900179.1900221.

[22] Xiaojuan Ning, Xiaopeng Zhang, and Yinghui Wang. Tree segmentation from scanned scene data. In PMA, December 2009. [Online]. Available:10.1109/PMA.2009.18.